Supplement of Atmos. Chem. Phys., 15, 1669–1681, 2015
http://www.atmos-chem-phys.net/15/1669/2015/
doi:10.5194/acp-15-1669-2015-supplement

Atmospheric Chemistry and Physics Open Access

Supplement of

Prediction of gas/particle partitioning of polybrominated diphenyl ethers (PBDEs) in global air: A theoretical study

Y.-F. Li et al.

Correspondence to: Y.-F. Li (ijrc_pts_paper@yahoo.com)

Contents

At a Glance 1

Supplementary Methods 3

S1. Fugacities and fugacity capacities 3

S2. Gas-particle partition equations at equilibrium state 3

Supplementary Figures 5

Supplementary Table 26

References 27

At a Glance

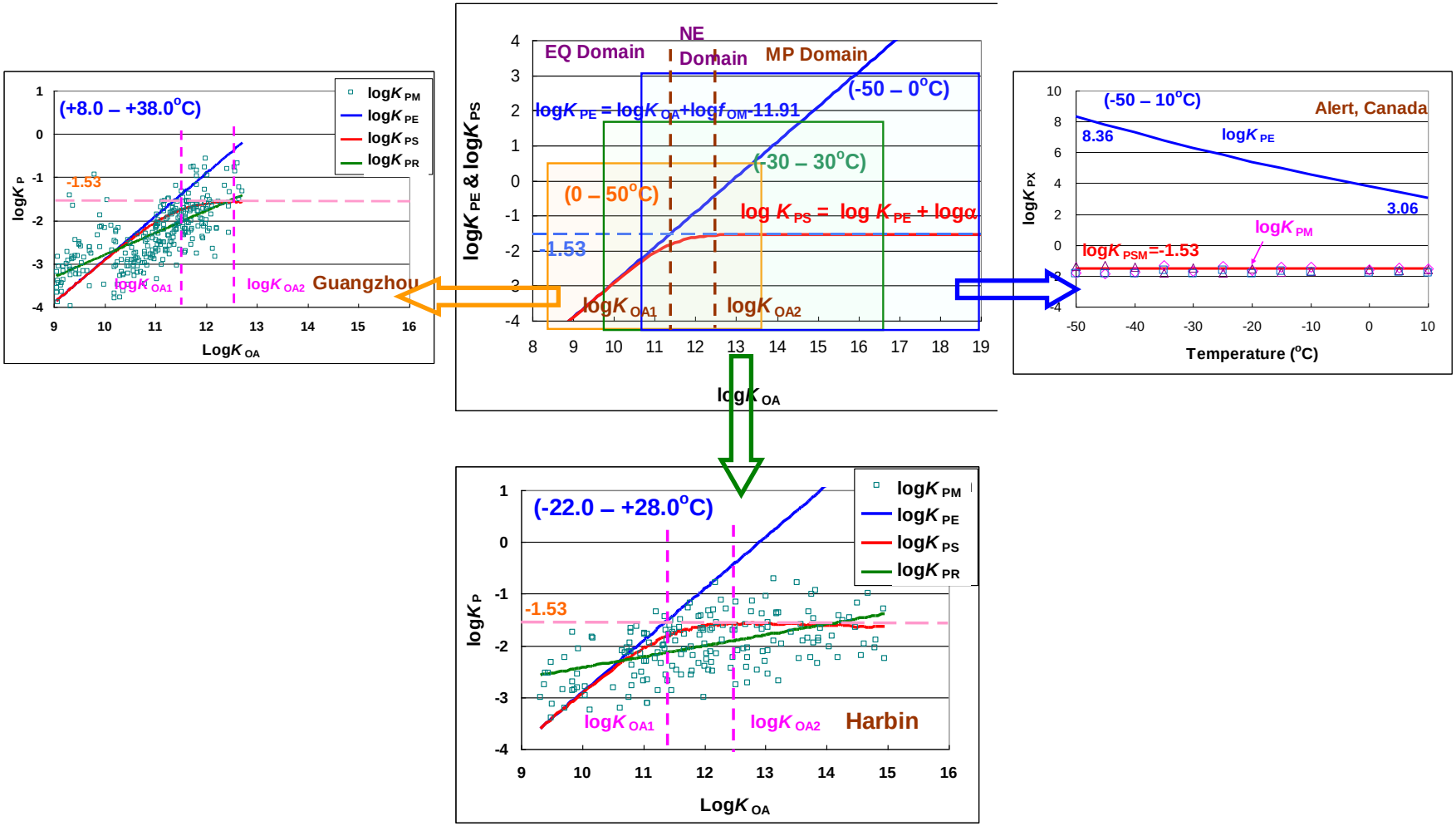
(+8.0 – +38.0°C)
logK PM
logK PE
logK PS
logK PR
-1.53
logK OA1
logK OA2
Guangzhou
logK P
Log K OA
EQ Domain
NE Domain
MP Domain
(-50 – 0°C)
logK PE = logK OA+logf OM-11.91
(-30 – 30°C)
(0 – 50°C)
log K PS = log K PE + logα
-1.53
logK OA1
logK OA2
logK PE & logK PS
logK OA
(-50 – 10°C)
Alert, Canada
8.36
logK PE
3.06
logK PM
logK PSM=-1.53
logK PX
Temperature (°C)
(-22.0 – +28.0°C)
logK PM
logK PE
logK PS
logK PR
-1.53
logK OA1
logK OA2
Harbin
logK P
Log K OA

G/P Partition coefficients of PBDEs in global air:

The top middle panel depicts the G/P partition coefficients of PBDEs as functions of logK_{OA} at environmental ambient temperature ranging from -50 to +50^{o}C, calculated by two equations. First one is G/P partition equation at equilibrium (Eq. (3)), presented by the dark blue straight line, and the second one is our newly developed G/P partition equation at steady state (Eq. (31)), presented by the red curve in the figure. Two threshold values of logK_{OA} (logK_{OA1} and logK_{OA2}, represented by two vertical pink dashed lines) divide the space of logK_{OA} into three domains: the equilibrium (EQ) domain, the nonequilibrium (NE) domain, and the maximum partition (MP) domain. Obvious difference in G/P partition coefficients between logK_{PS} and logK_{PE} can be observed when logK_{OA} ≥ logK_{OA1}, and becomes larger when the values of logK_{OA} increases. One appealing result is that, our new equation leads to a conclusion that the G/P partition coefficients reach a maximum value of logK_{PS} (logK_{PSM} = -1.53, represented by the horizontal light blue line) when logK_{OA} ≥ logK_{OA2}maximum partition. The three squares in the panel designate the logK_{P}-logK_{OA} graphs with three different temperature zones: 0 – +50^{o}C, -30 – +30^{o}C, and -50 – 0^{o}C, representing the tropical and subtropical climate zones, warm temperate climate zone, and boreal and tundra climate zones, respectively. Monitoring data (logK_{PM}), their regression data (logK_{PR}), and the predicted results logK_{PS} and logK_{PE} in Guangzhou, China (Yang et al. 2013), within the subtropical climate zone, shown in the top-left panel, and those in Harbin, China (Yang et al. 2013), within the warm temperate climate zone, shown in the bottom panel indicating that the curve of our new equation (logK_{PS}) is closer to the line of logK_{PR} than logK_{PE}. The top-right panel gives the predicted results logK_{PSM} and logK_{PE} of BDE-209 in Alert, Canada, which is an Arctic sampling site in tundra climate zone. The monitoring data of BDE-209 (logK_{PM}) for three years from 2007 to 2009 by Environment Canada (NCP 2013), denoted by the diamond, square, and triangle marks, match our predicted data (logK_{PSM} = -1.53) extremely well (assuming TSP = 10 μg m^{-3}). All these indicate that the steady equation (logK_{PS}) is superior than the equilibrium equation (logK_{PE}) in G/P prediction of partitioning behavior for PBDEs in air.

Supplementary Methods

S1. Fugacities and fugacity capacities (Mackay 2001)

The fugacity *f* is a measure of a SVOC (a PBDE congener, for example) escaping tendency from a particular medium; and SVOCs tend to move from medium where it has higher fugacity to medium where it has lower fugacity. Fugacity is proportional to concentration in the medium and given by

$$f_I = C_I / Z_I \quad \text{(S1)}$$

where the subscript "I" indicates the medium I, and C_I is the concentration (in mol/m^3 of medium I) of a SVOC. The fugacity capacity Z_I (*Z*-value, mol m^{-3} Pa^{-1}) describes the potential of a medium I to retain a SVOC.

The *Z*-value for air is given by

$$Z_G = 1/RT \quad \text{(S2)}$$

where *R* is the gas constant (8.314 Pa $m^3 mol^{-1} K^{-1}$), and *T* is air temperature in K.

The fugacity capacity for particles is given by

$$Z_P = K_{PG} Z_G \quad \text{(S3)}$$

$$Z_P = K_{PG}/RT \quad \text{(S4)}$$

where K_{PG} is dimentionless partition coefficient of a SVOC between gas- and particle-phases at equilibrium.

S2. Gas-particle partition equations at equilibrium state

At equilibrium, the fugacities of a chemical in gas-phase (f_G) and in particle-phase (f_P) are equal,

$$f_G = f_P \quad \text{(S5)}$$

where,

$$f_G = C_G / Z_G \quad \text{(S6a)}$$

$$f_P = C'_P / Z_P \quad \text{(S6b)}$$

In the above equations, Z_G and Z_P are given by Eqs. (S2) and (S4), respectively, and C_G is the concentration of the comical in gas phase (mol m^{-3} of air), while C'_P is concentration in particle phase (mol m^{-3} of *particles*). Equations (S7) gives the relationship between C_G and C'_P *at equilibrium*,

$$C'_P / C_G = Z_P / Z_G = K_{PG} \quad \text{(at equilibrium)} \quad \text{(S7)}$$

The G/P partition coefficient of SVOCs has another more commonly used form, K_{PE}, defined as

$$K_{PE} = (C_P / TSP) / C_G \quad \text{(at equilibrium)} \quad \text{(S8)}$$

where C_G and C_P are concentration of SVOCs in gas- and particle-phases (both in mol m^{-3} of *air*), respectively, *at equilibrium*, and *TSP* is the concentration of total suspended particle in air (μg m^{-3}). Thus K_{PE} has a unit of $m^3 \mu g^{-1}$, the reciprocal unit of *TSP*. Harner and Bidleman (1998) derived the following equation to calculate K_{PE},

$$\log K_{PE} = \log K_{OA} + \log f_{OM} - 11.91 \quad \text{(S9)}$$

where f_{OM} is organic matter content of the particles.

The relationship between K_{PG} and K_{PE} is given by

$$K_{PG} = 10^9 \rho(\text{kg } m^{-3}) \, K_{PE}(m^{-3} \mu g) \quad \text{(S10)}$$

where ρ is density of particles in the unit of kg m^{-3}. The relationship between C'_P and C_P is given by

$$C'_P \text{ (pg } m^{-3} \text{ of } particle) = 10^9 \rho(\text{kg } m^{-3}) \, C_P \text{ (pg } m^{-3} \text{ of } air) / TSP(\mu g \, m^{-3}) \quad \text{(S11)}$$

Supplementary Figures

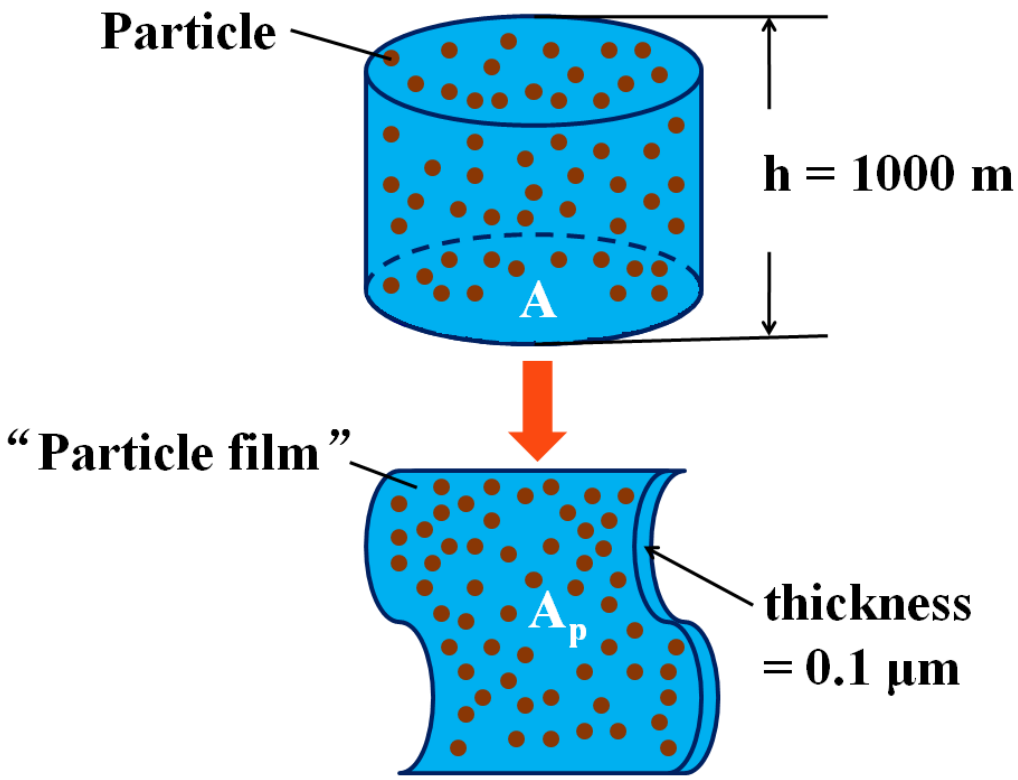

Figure S1: Particles are treated as a “particle film”.

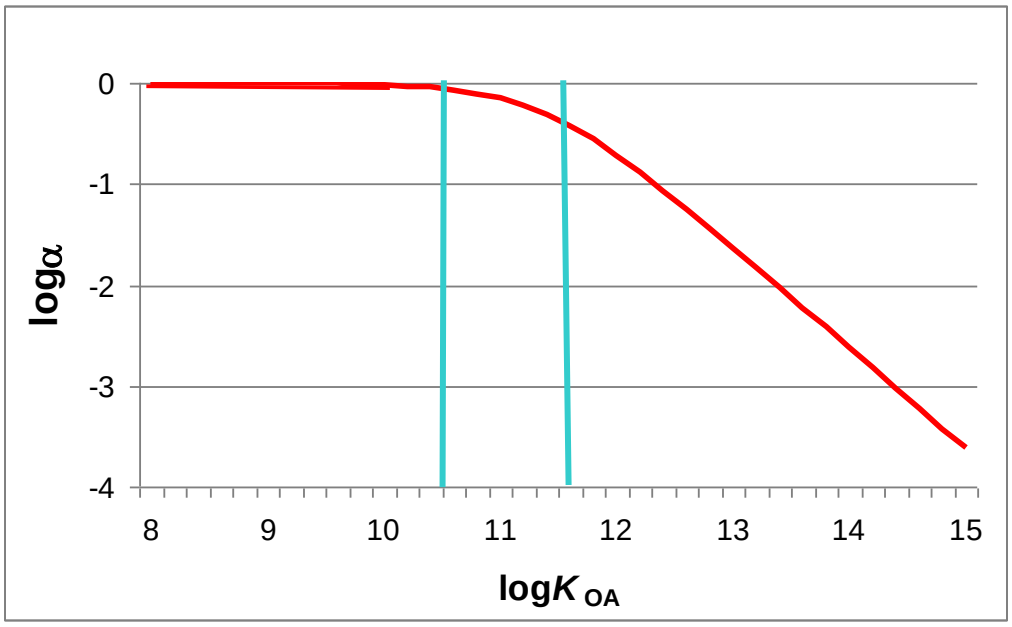

(A)

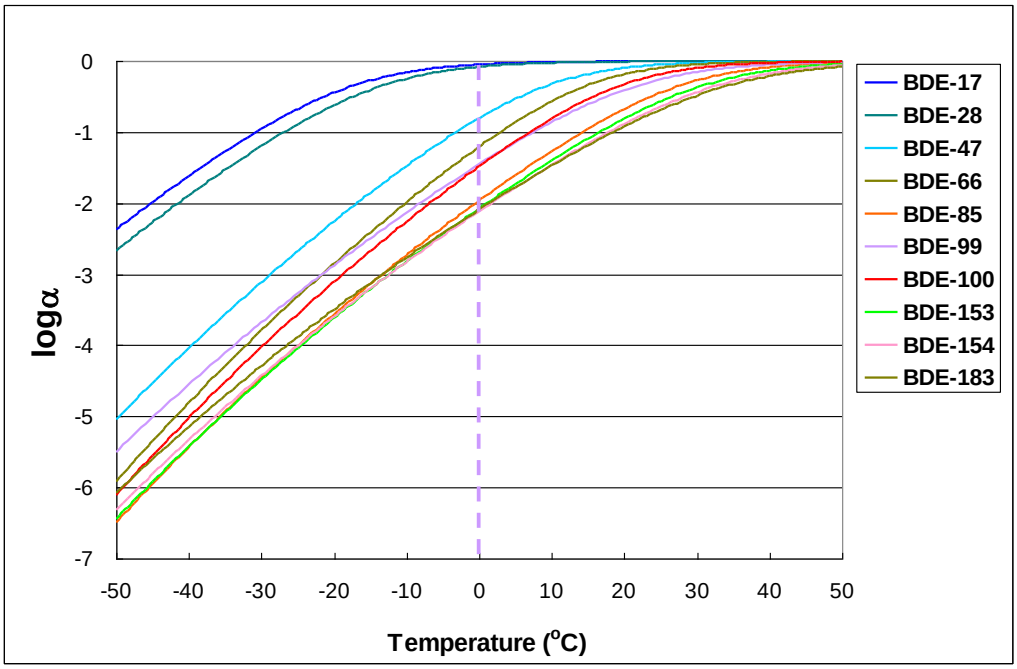

(B)

Figure S2: Variation of log*a* as functions of (**A**) logK_{OA} and (**B**) temperature for 10 PBDE congeners (C=5).

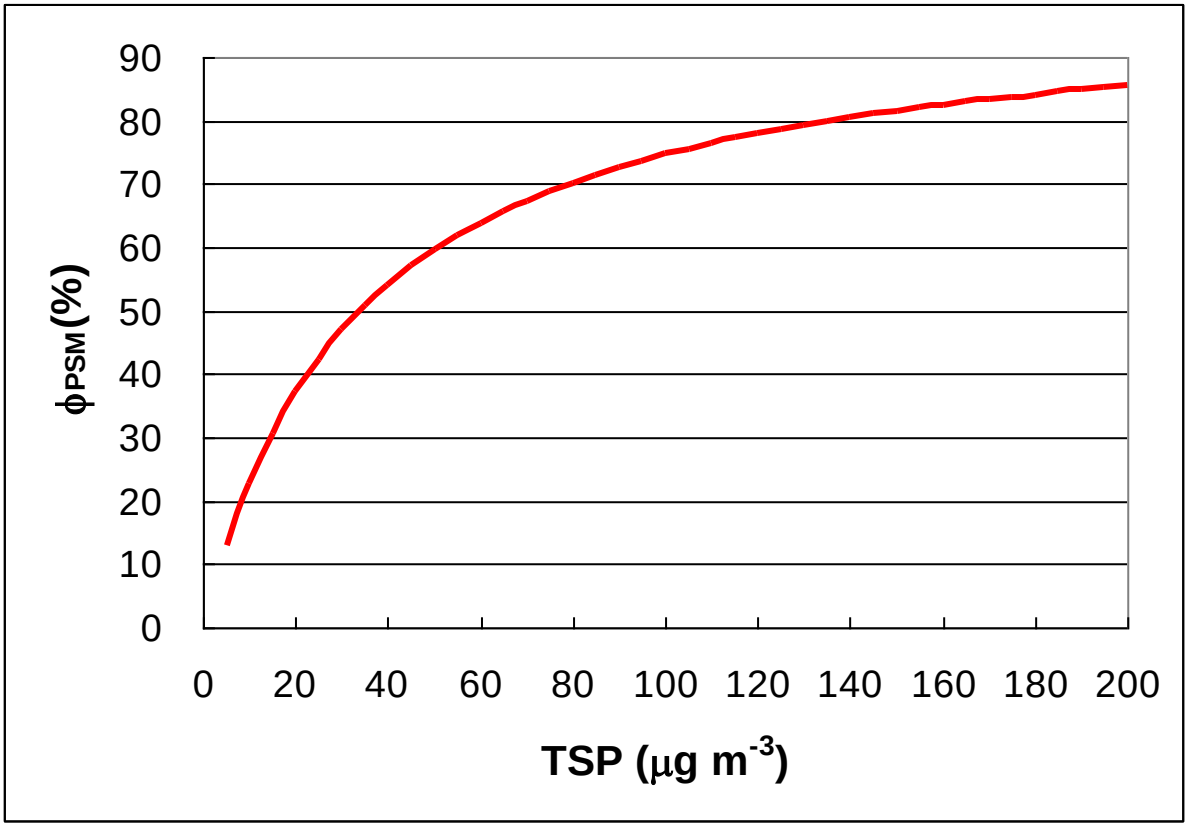

Figure S3: The maximum particle phase fraction as a function of *TSP*. While $\log K_{PSM}$ = -1.53 is a constant, ϕ_{PSM} is a function of *TSP*.

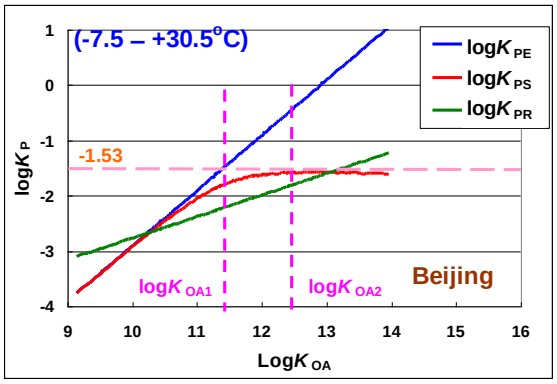
(-7.5 – +30.5°C)
logK PE
logK PS
logK PR
-1.53
logK OA1
logK OA2
Beijing
logK P
LogK OA

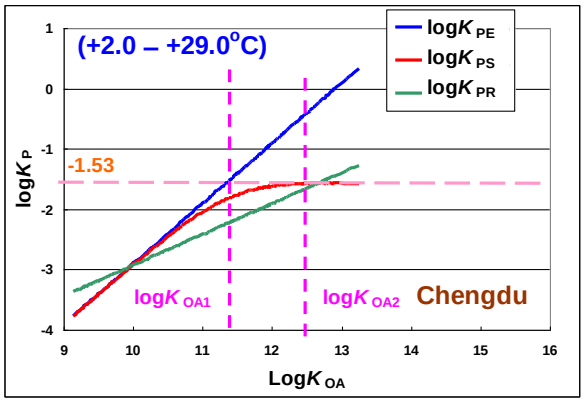
(+2.0 – +29.0°C)
logK PE
logK PS
logK PR
-1.53
logK OA1
logK OA2
Chengdu
logK P
LogK OA

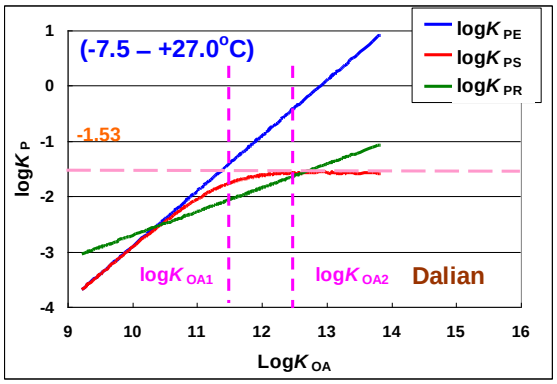
(-7.5 – +27.0°C)
logK PE
logK PS
logK PR
-1.53
logK OA1
logK OA2
Dalian
logK P
LogK OA

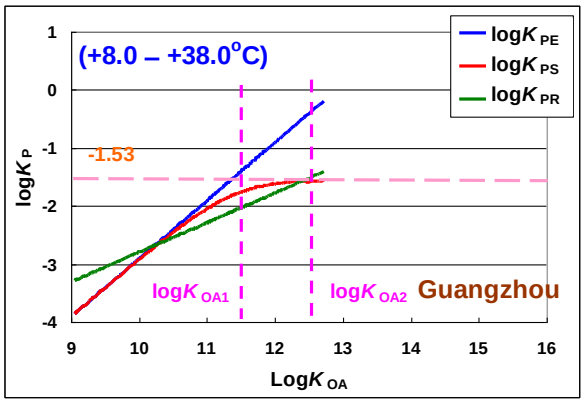
(+8.0 – +38.0°C)
logK PE
logK PS
logK PR
-1.53
logK OA1
logK OA2
Guangzhou
logK P
LogK OA

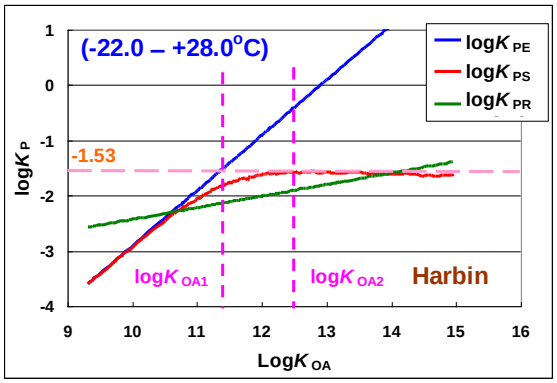
(-22.0 – +28.0°C)
logK PE
logK PS
logK PR
-1.53
logK OA1
logK OA2
Harbin
logK P
LogK OA

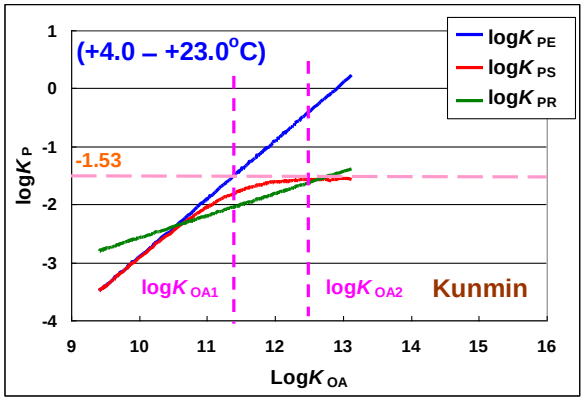
(+4.0 – +23.0°C)
logK PE
logK PS
logK PR
-1.53
logK OA1
logK OA2
Kunmin
logK P
LogK OA

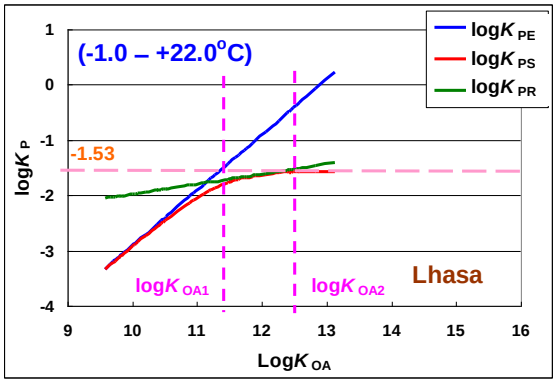
(-1.0 – +22.0°C)
logK PE
logK PS
logK PR
-1.53
logK OA1
logK OA2
Lhasa
logK P
LogK OA

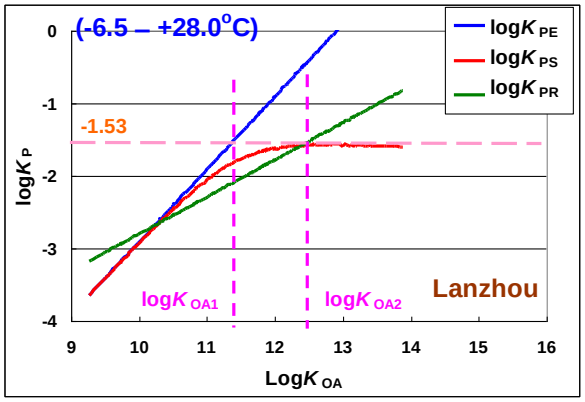
(-6.5 – +28.0°C)
logK PE
logK PS
logK PR
-1.53
logK OA1
logK OA2
Lanzhou
logK P
LogK OA

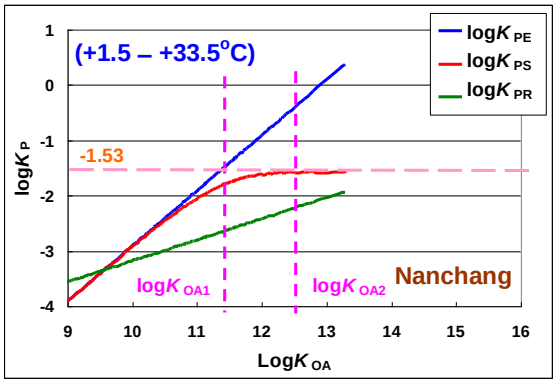

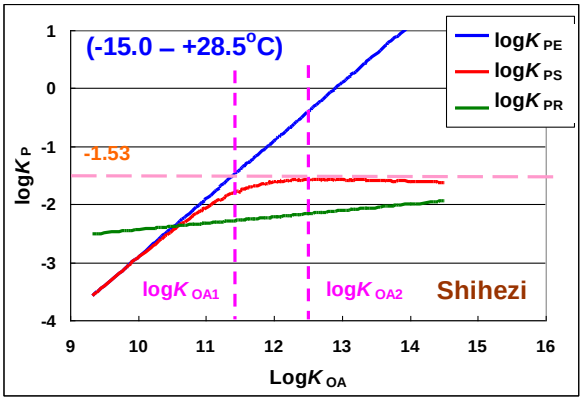

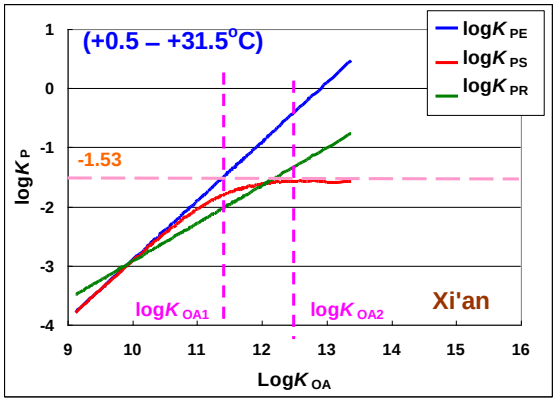

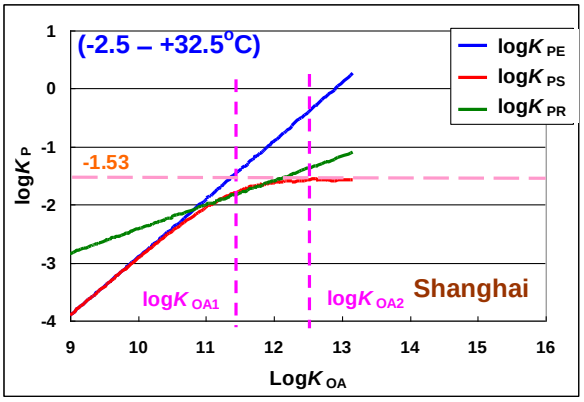

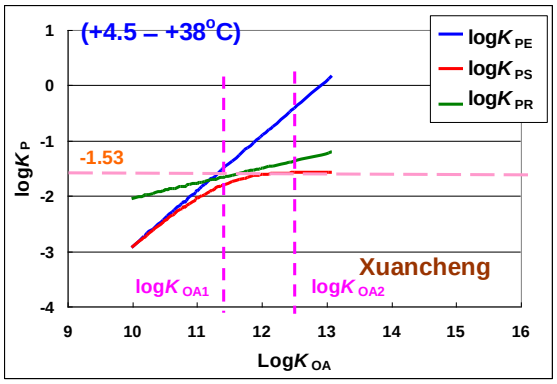

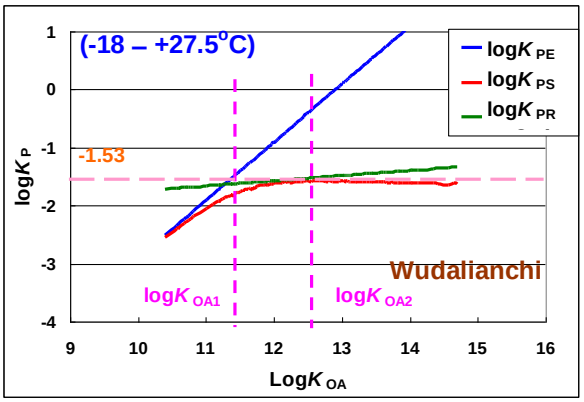

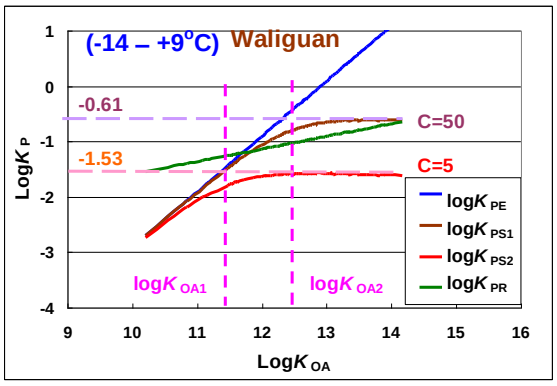

Figure S4: Variations of logK_{PS}, logK_{PE}, and logK_{PR} as functions of logK_{OA} for 15 sampling sites. Red lines are for logK_{PS} from Equation (31) under steady state; blue lines for logK_{PE} from Equation (3) under equilibrium state. (C = 5 at all sampling sites but Waliguan, where C = 50) (Data for logK_{PR}: Yang et al., 2013).

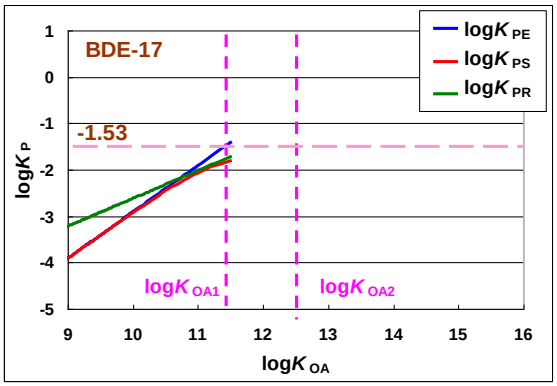
BDE-17
-1.53
logK PE
logK PS
logK PR
logK OA1
logK OA2
logK P
logK OA

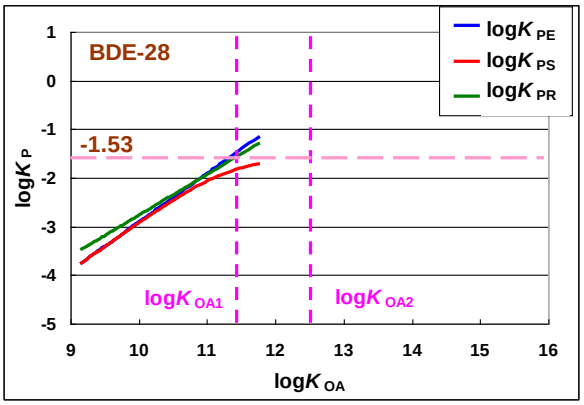
BDE-28
-1.53
logK PE
logK PS
logK PR
logK OA1
logK OA2
logK P
logK OA

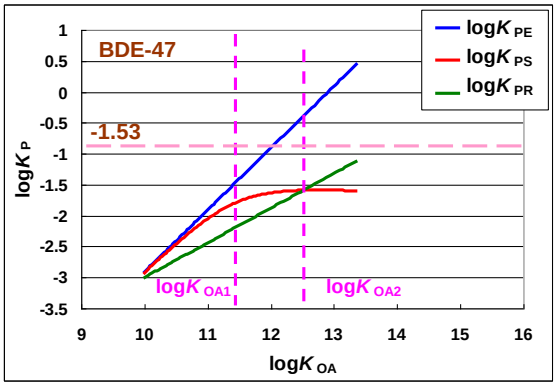
BDE-47
-1.53
logK PE
logK PS
logK PR
logK OA1
logK OA2
logK P
logK OA

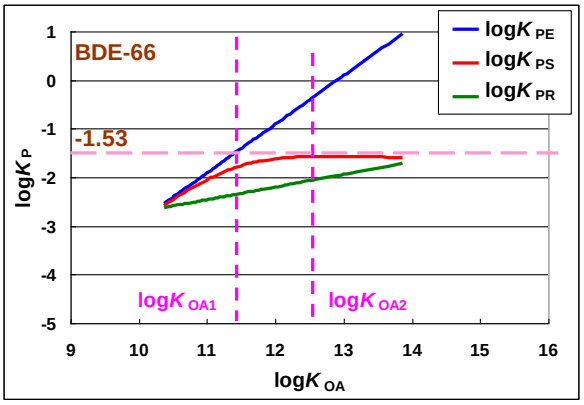
BDE-66
-1.53
logK PE
logK PS
logK PR
logK OA1
logK OA2
logK P
logK OA

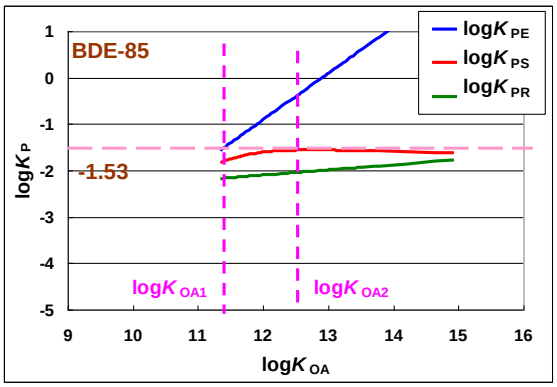
BDE-85
-1.53
logK PE
logK PS
logK PR
logK OA1
logK OA2
logK P
logK OA

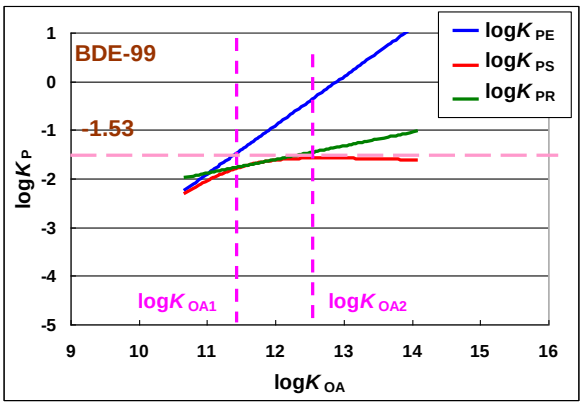
BDE-99
-1.53
logK PE
logK PS
logK PR
logK OA1
logK OA2
logK P
logK OA

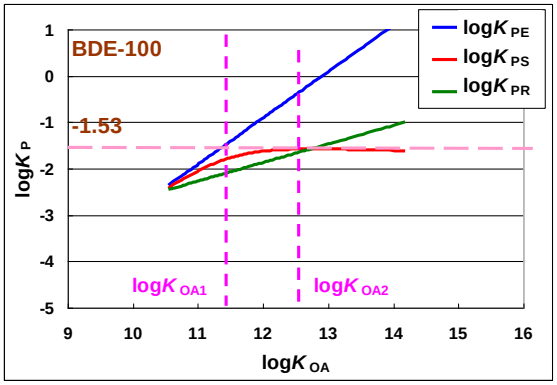
BDE-100
-1.53
logK PE
logK PS
logK PR
logK OA1
logK OA2
logK P
logK OA

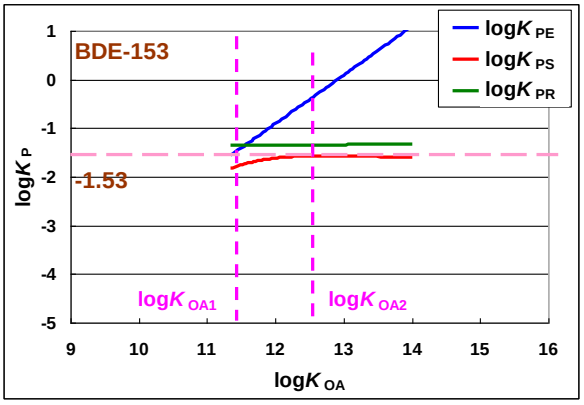
BDE-153
-1.53
logK PE
logK PS
logK PR
logK OA1
logK OA2
logK P
logK OA

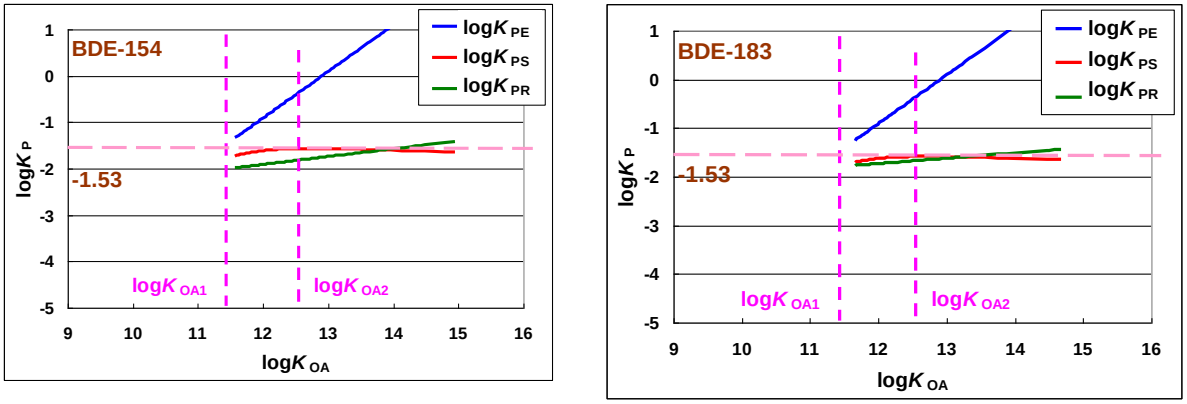

Figure S5: Comparisons among the predicted K_{PS} values using Equation (31), predicted K_{PE} values using Equation (3), and the regression K_{PR} values using Equation (2) as functions of logK_{OA} for the 10 PBDE congeners (Data for logK_{PR}:Yang et al., 2013).

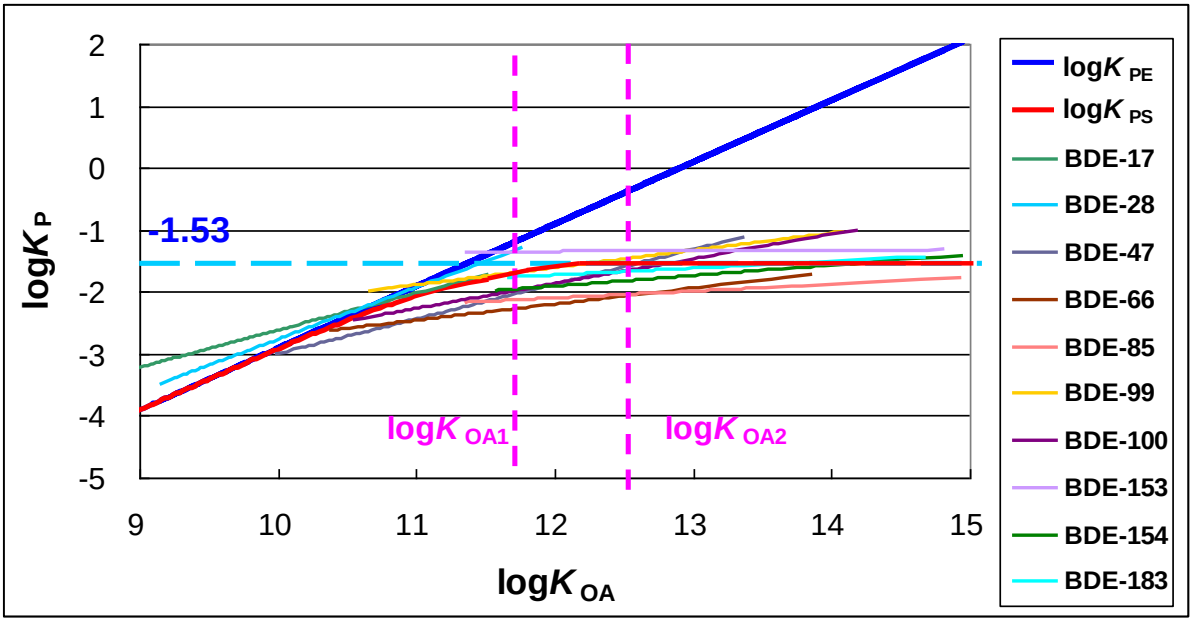

Figure S6: The regression curves ($\log K_{PR}$) for the 10 PBDE congeners from Figure S5 along with the curves of $\log K_{PE}$ and $\log K_{PS}$, indicating that these 10 lines of $\log K_{PR}$ change their slopes m_O along the curve of $\log K_{PS}$, not the straight line of $\log K_{PE}$.

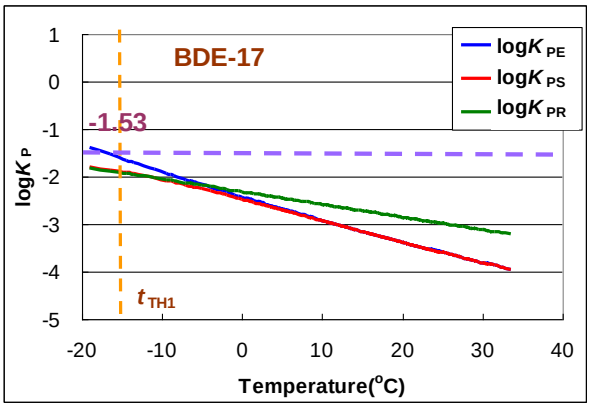
BDE-17
logK PE
logK PS
logK PR
-1.53
t TH1
logK P
Temperature(°C)

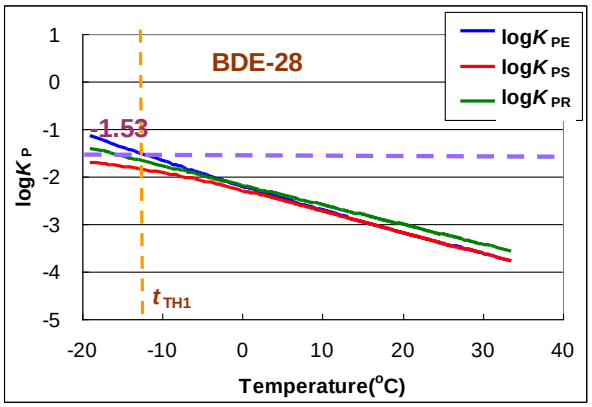
BDE-28
logK PE
logK PS
logK PR
-1.53
t TH1
logK P
Temperature(°C)

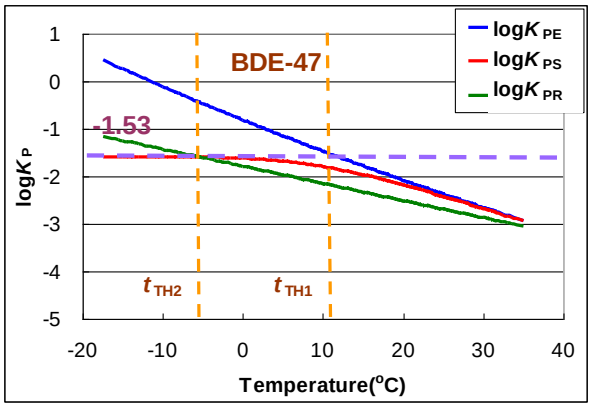
BDE-47
logK PE
logK PS
logK PR
-1.53
t TH2
t TH1
logK P
Temperature(°C)

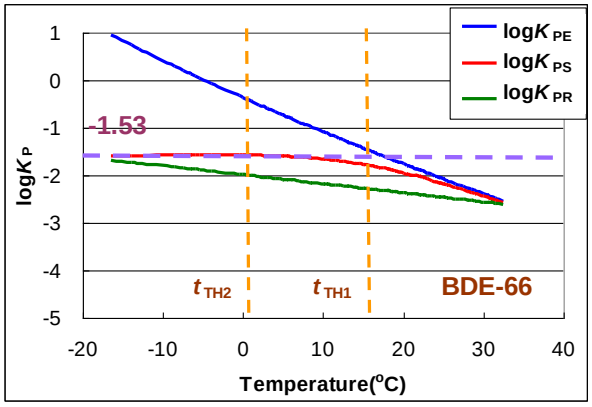
BDE-66
logK PE
logK PS
logK PR
-1.53
t TH2
t TH1
logK P
Temperature(°C)

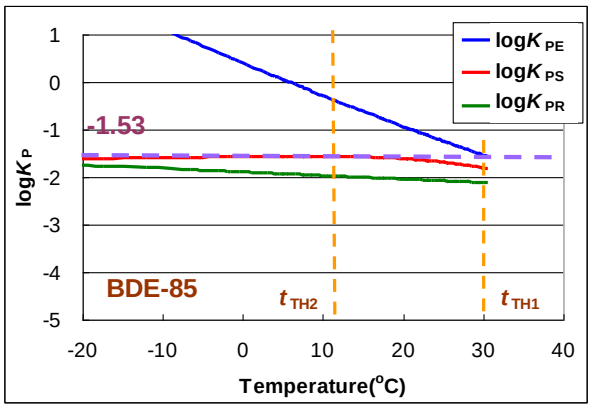
BDE-85
logK PE
logK PS
logK PR
-1.53
t TH2
t TH1
logK P
Temperature(°C)

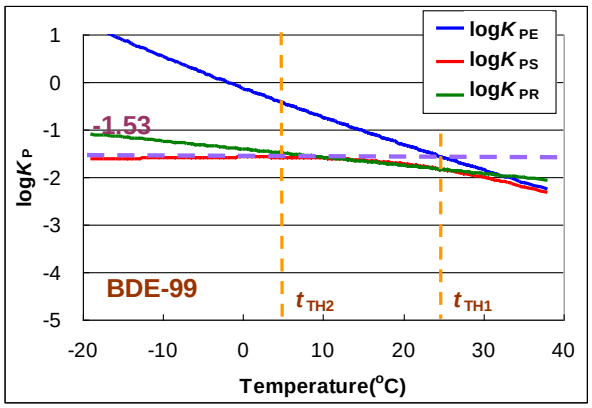
BDE-99
logK PE
logK PS
logK PR
-1.53
t TH2
t TH1
logK P
Temperature(°C)

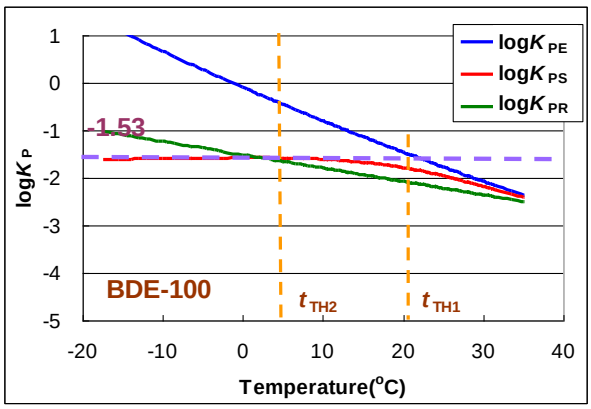
BDE-100
logK PE
logK PS
logK PR
-1.53
t TH2
t TH1
logK P
Temperature(°C)

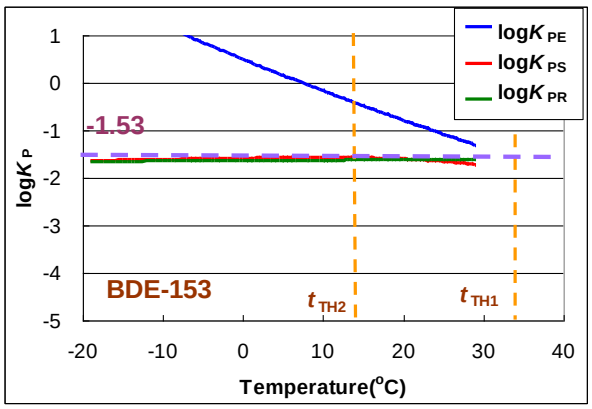
BDE-153
logK PE
logK PS
logK PR
-1.53
t TH2
t TH1
logK P
Temperature(°C)

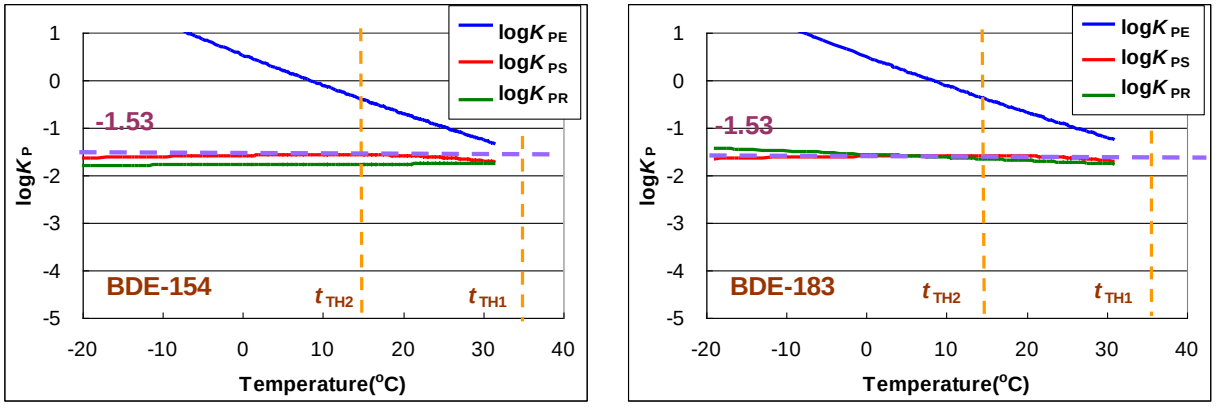

Figure S7: Variations of logK_{PS}, logK_{PE}, and logK_{PR} as functions of temperature for 10 PBDE congeners. Red lines are for logK_{PS} from Equation (31) under steady state; blue lines for logK_{PE} from Equation (3) under equilibrium state; and green lines are for logK_{PR} from Equation (2). These figures indicate that, the curve of logK_{PS} matches the line of logK_{PR} for each PBDE congener, the high brominated congeners in particular, dramatically well (Data for logK_{PR} were from Yang et al., 2013).

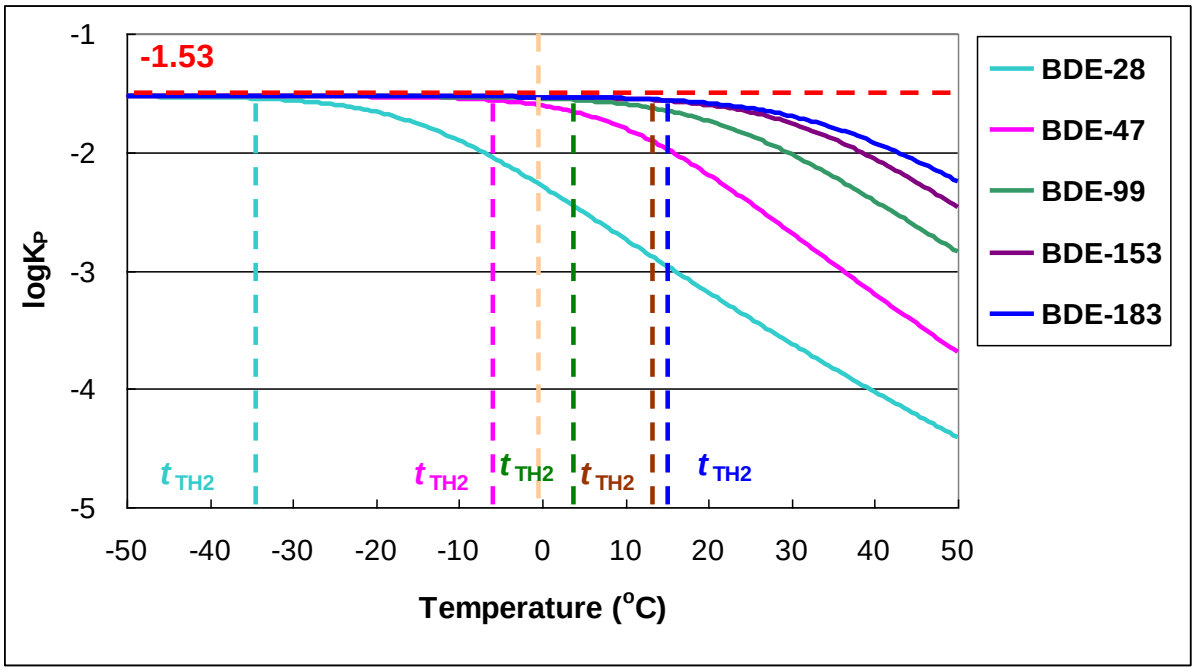

Figure S8: The modeled values of logK_{PS} for typical 5 PBDE congeners as functions of temperature. Along with decrease of temperature, the values of logK_{PS} for each PBDE congener increases to the maximum partition value (-1.53). The second threshold temperatures (t_{TH2}), are also show.

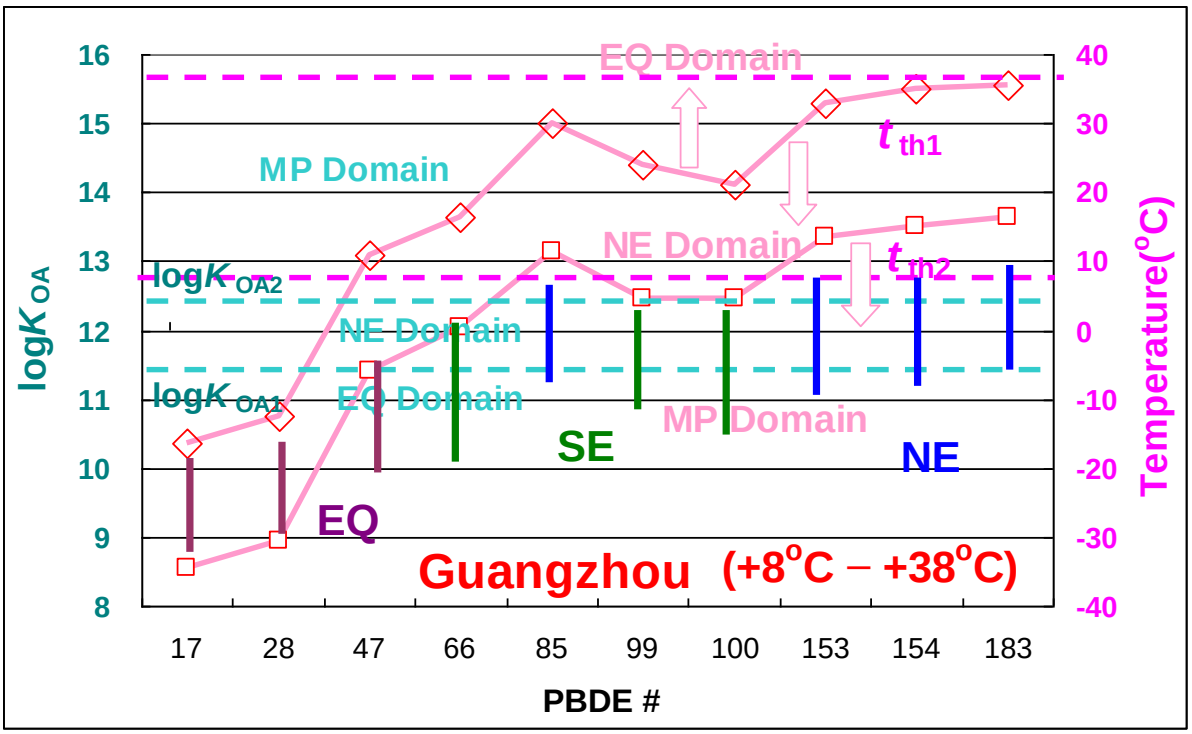

Figure S9: The range of logK_{OA} for 10 PBDE congeners (vertical bars) in Guangzhou air with a temperature range from +8 to +38 ^{o}C and the 2 light blue horizontal dashed lines give the 2 threshold values of logK_{OA1} and logK_{OA2}, which divide the space of logK_{OA} (the left axis) into three domains: the equilibrium (EQ), the nonequilibrium (NE), and the maximum partition (MP) domains. The minimum and the maximum temperatures (+8^{o}C and +38^{o}C) in Guangzhou (the red dashed lines) and the two threshold temperatures, t_{TH1} (the red diamonds) and t_{TH2} (the red squares) for the 10 PBDE congeners (the right axis) are also presented in the figure. The lines of t_{TH1} and t_{TH2} also divide the temperature space (the right axis) into the same 3 domains. The PBDE congeners in Guangzhou air can be segregated into 3 groups; BDE-17, -28, and -47 as equilibrium EQ-group, BDE-66, -99, and -100 as semiequilibrium SE-group, and the others as nonequilibrium NE-group.

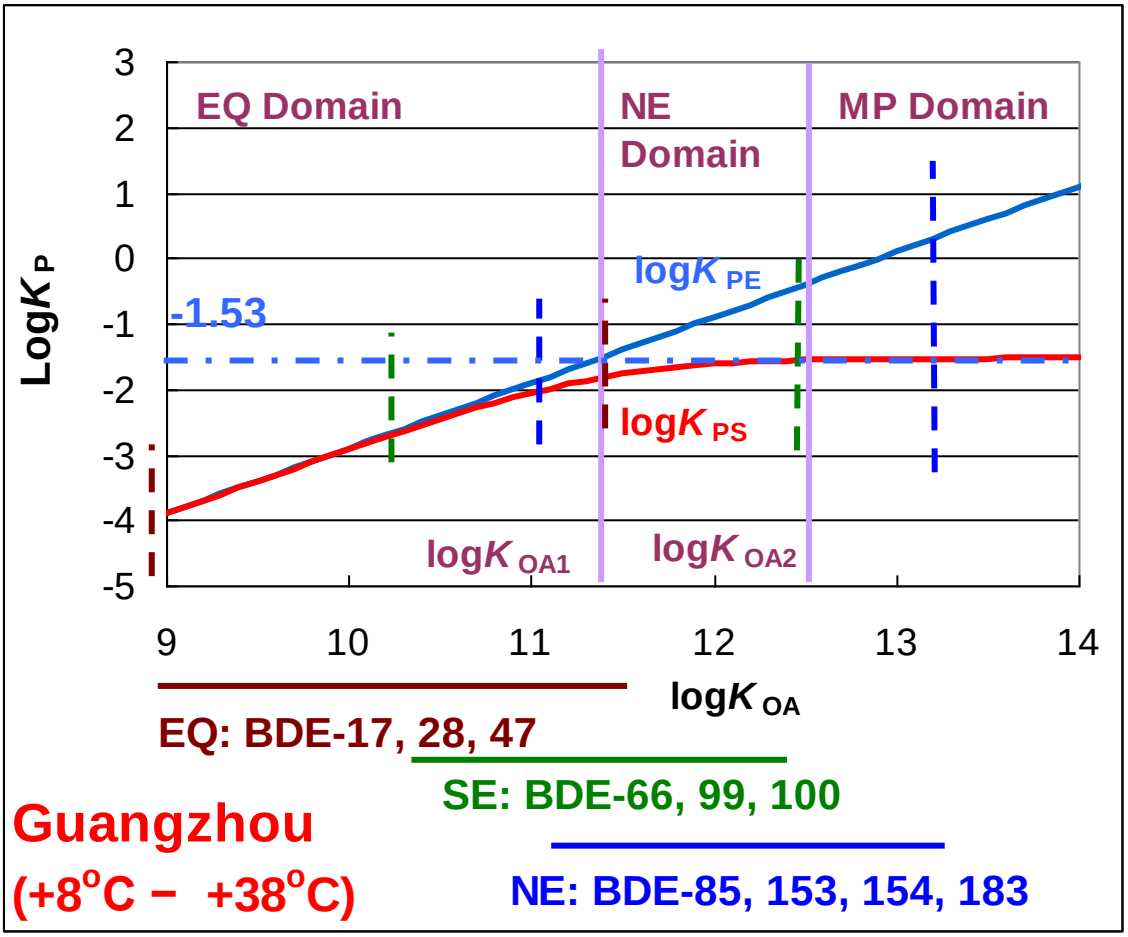

Figure S10. The logK_P - logK_{OA} diagram for PBDEs in Guangzhou air. The range of logK_{OA} for each group and their corresponding logK_P - logK_{OA} diagram are also shown. The logK_P - logK_{OA} diagram for the EQ Group, boned by 2 purple dashed lines, is mainly in the EQ domain; the logK_P - logK_{OA} diagram for the SE Group, contained by 2 green dashed lines, is mainly in the NE domain; and the logK_P - logK_{OA} diagram for the NE Group, formed by the 2 blue dashed lines, is mainly in the NE and MP domains.

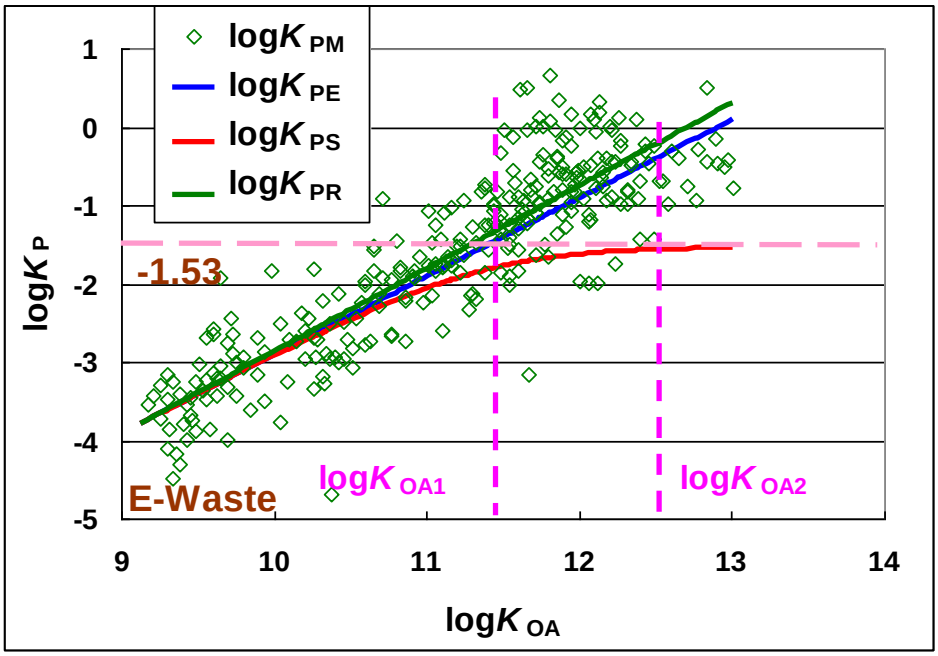

(A)

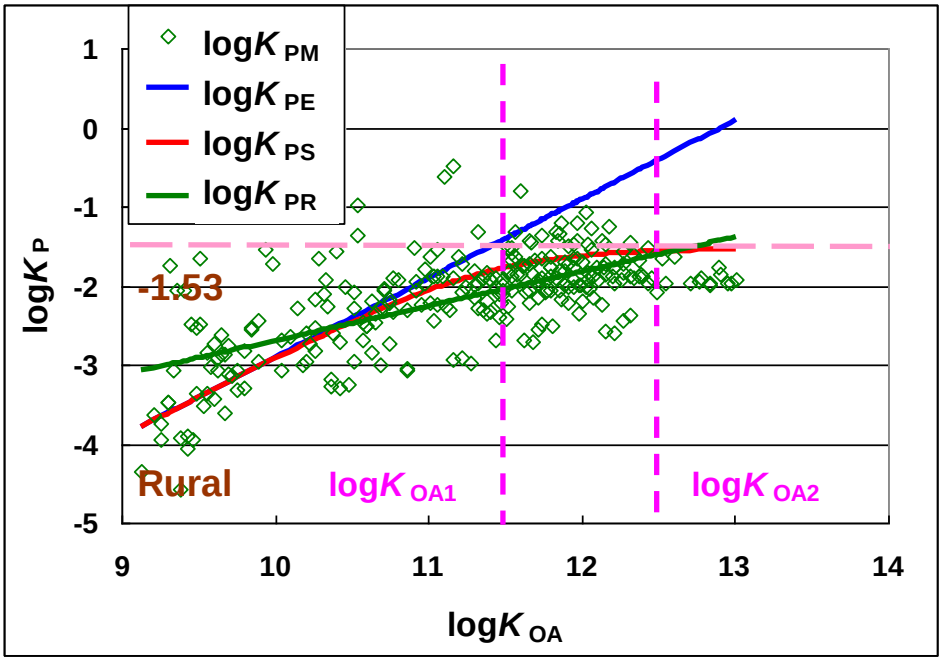

(B)

Figure S11: Variation of logK_{PE}, logK_{PS}, logK_{PR}, and logK_{PM} as functions of logK_{OA} at (A) an e-waste site and (B) a rural site. Two threshold values of logK_{OA} are also shown. (Monitoring data were from Tian et al. 2011).

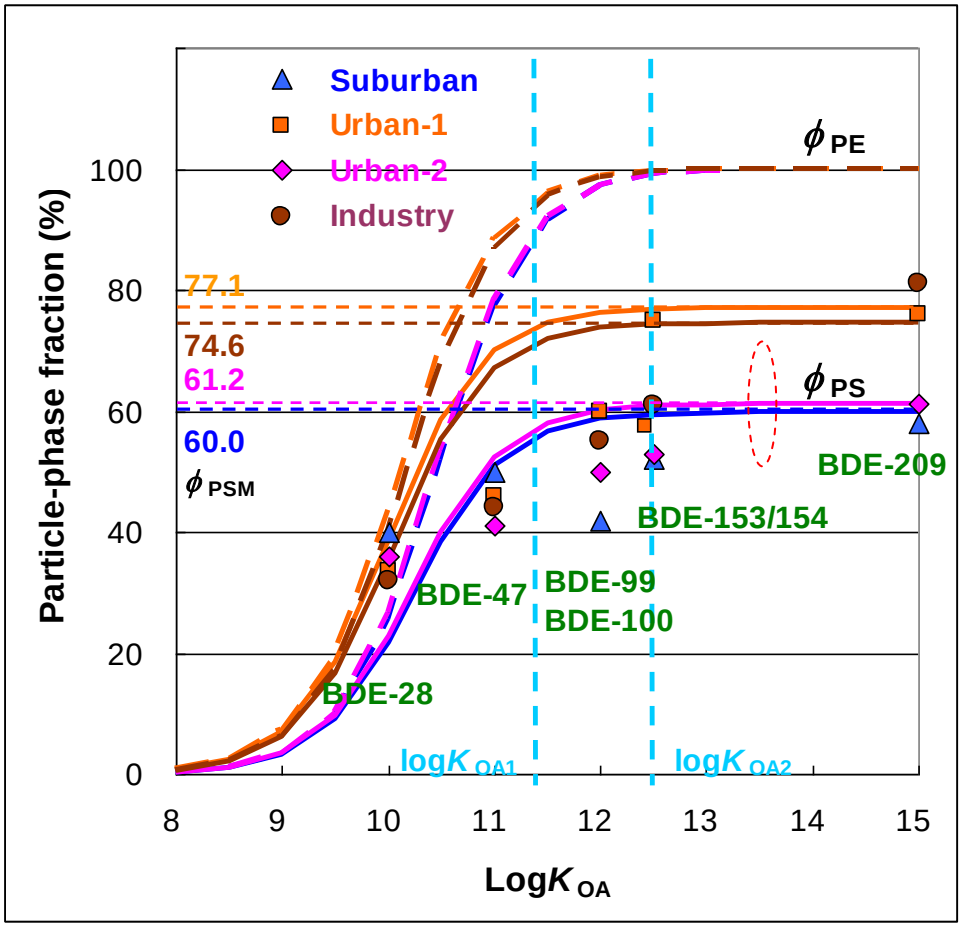

Figure S12: Variation of particle fractions as functions of logK_{OA} for 7 PBDE congeners (BDE-28, -47, -99, -100, -153, -154 and -209) at four sites (1 suburban, 2 urban, and 1 industrial) in Izmir, Turkey in summer and winter in 2004-2005 with a temperature range between 1.8°C and 22.4°C. The monitoring data are from (Cetin and Odabasi, 2007). The four different colors design 4 different site types. The solid lines are for ϕ_{PS} and the dashed lines for ϕ_{PE}. Two threshold values of logK_{OA} and the maximum values of particle fractions ϕ_{PSM} are also shown. The modeled particle fractions ϕ_{PS} and ϕ_{PE} are compared with the monitoring data. Different from the figure by (Cetin and Odabasi, 2007), there are four lines of ϕ_{PE} in this figure caused by different values of *TSP*. It is obvious that the results of our steady model (ϕ_{PS}) can make a better prediction on the particle fractions than equilibrium model (ϕ_{PE}). It is noticed that although the maximum values of logK_{PSM} are same at the 4 sites, all equal to -1.53, the maximum values of ϕ_{PSM} are different due to different concentration of *TSP* for the 4 sampling sites. The concentration of *TSP* in the four sites were (in μg/m^3), suburban: 50.5; urban-1: 114; urban-2: 53.5; and industrial: 99.5. The value of 0.55 was used for f_{OM} at the four sites. It is interesting to note that the best agreement was observed for BDE-209. The monitoring data of PBDEs were corrected to 25 ℃ by Cetin and Odabasi, (2007).

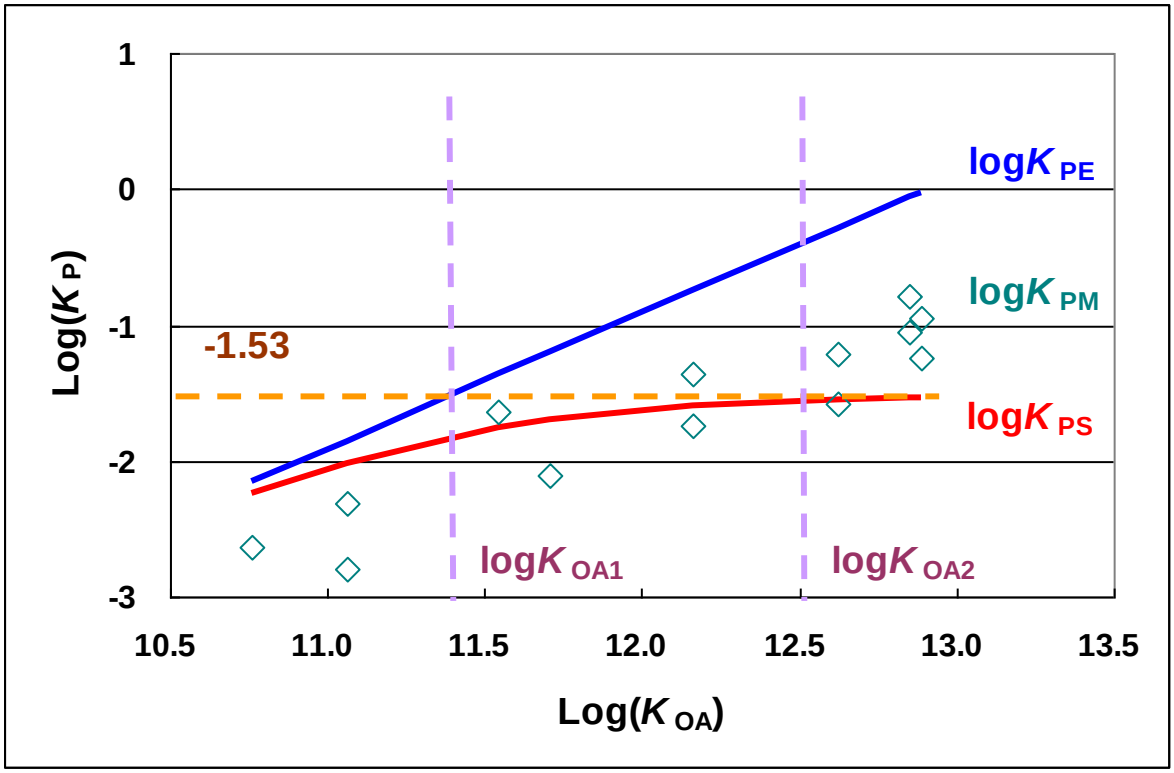

Figure S13: Variation of logK_{PE}, logK_{PS}, and logK_{PM} as functions of logK_{OA} for PBDEs in atmosphere of Kyoto, Japan, measured in August 2000, January and September 2001 (The monitoring data are from Hayakawa et al. (2004)). The two threshold values of logK_{OA} are also shown.

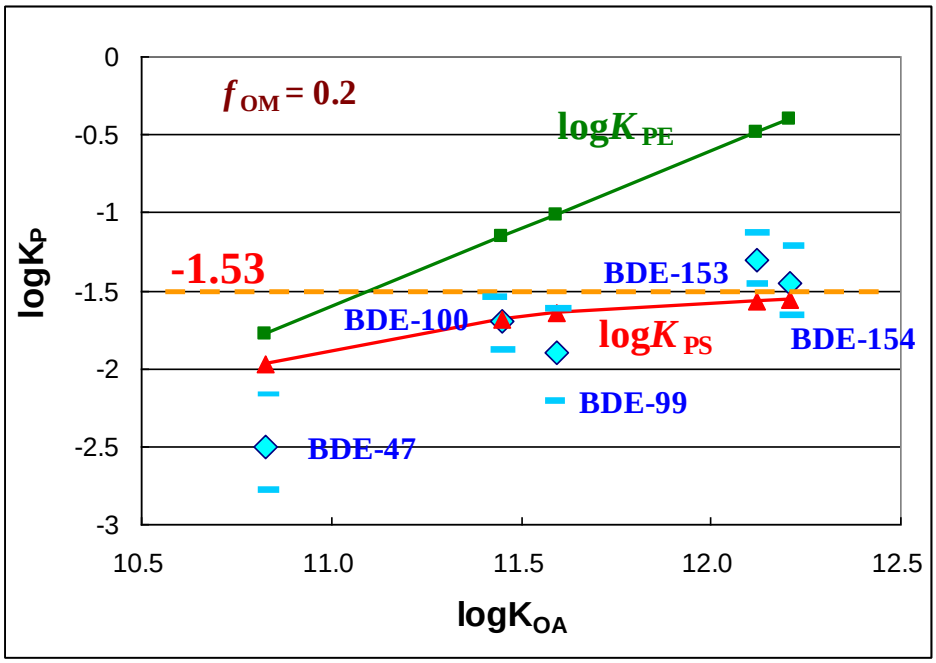

(A)

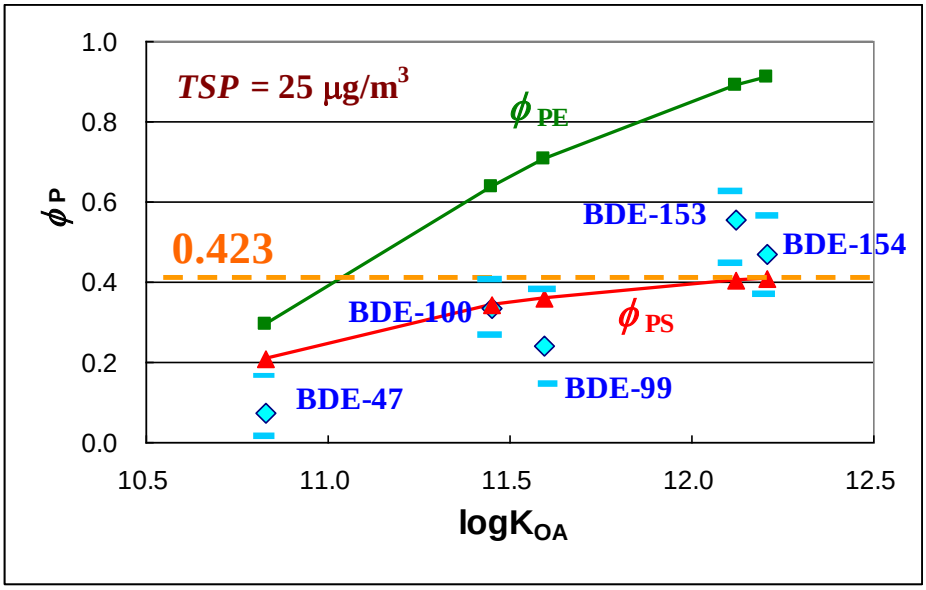

(B)

Figure S14: Partition coefficients **(A)** and particle fraction **(B)** of 5 PBDE congeners (BDE-47, -99, -100, -153, and -154) in air of the Great Lakes from Strandberg et al. (2001) along with predicted data using Eqs. (3) and (41) for equilibrium and Eqs. (31) and (41) for steady state at 20 ℃ as functions of logK_{OA}. The values of logK_{OA} for the 5 PBDE congeners were calculated by using Eq. (7) with t= 20 ℃. The typical values of f_{OM} = 0.2 and TSP = 25 μg m^{-3} suggested by Harner and Shoeib (2002) were used for calculation.

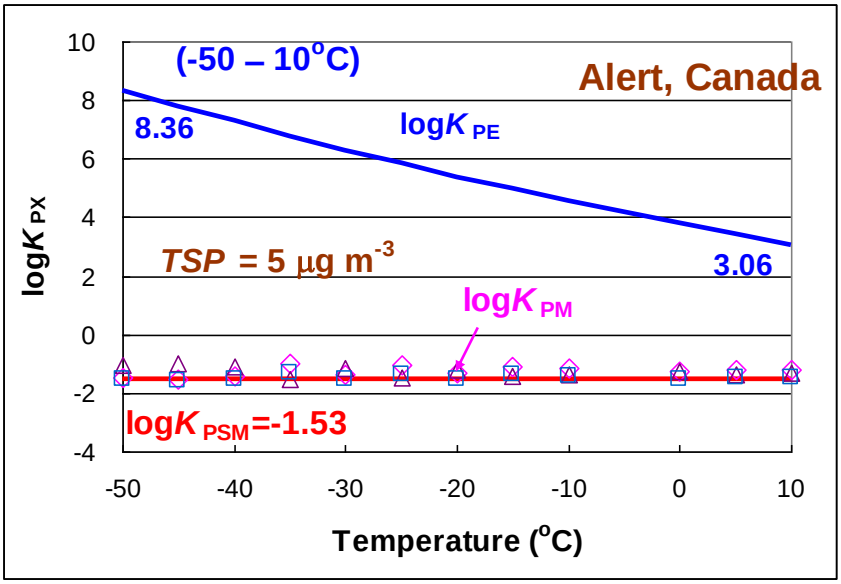

(A)

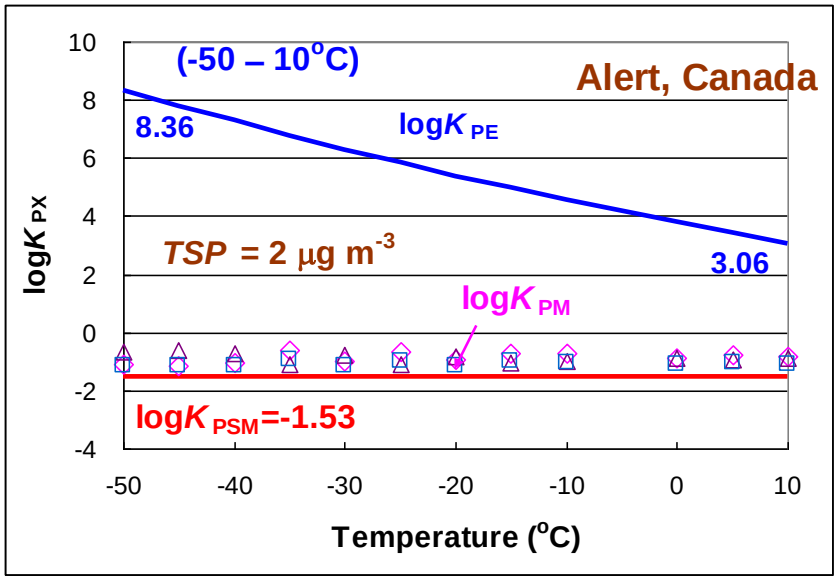

(B)

Figure S15: The results of logK_{PSM} and logK_{PE} of BDE-209 at an Arctic sampling site, Alert, Canada as functions of temperature. The monitoring data of BDE-209 (logK_{PM}) for three years from 2007, 2008, and 2009 by Environment Canada (NCP 2013), denoted by the diamond, square, and triangle marks, respectively, matched our predicted data (logK_{PSM} = -1.53) well. (**A**) *TSP* = 5 μg m^{-3}, (**B**) *TSP* = 2 μg m^{-3}. In order to calculate logK_{PE} for BDE-209, we used the value of 14.98 at 25 °C by Cetin and Odabasi (2007), and assumed that the variation of logK_{OA} for BDE-209 is the same as BDE-183.

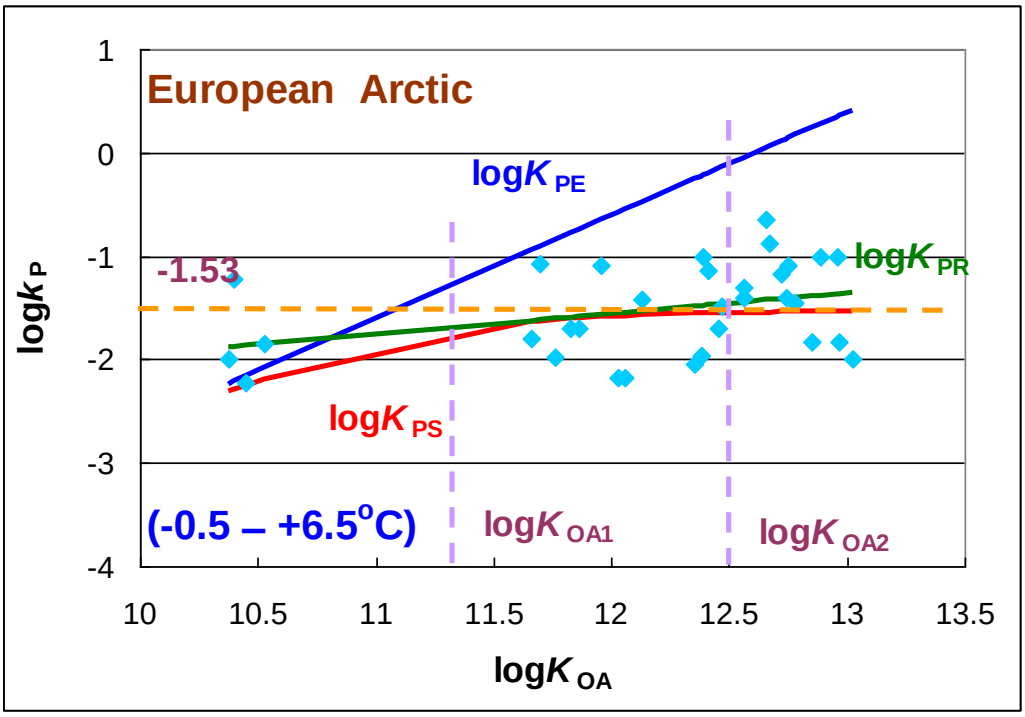

Figure S16: The values of logK_{PS}, logK_{PE}, and logK_{PR} as functions of logK_{OA}. The two threshold values of logK_{OA} are also shown. It is clearly shown that the data of logK_{PS} (the red line) matched the data of both logK_{PM} (the blue diamonds) and logK_{PR} (the green line) better than the equation of logK_{PE} (the blue line), especially for those congeners in the nonequilibrium domain with logK_{OA} > logK_{OA1}. The monitoring data are from Möller et al (2011).

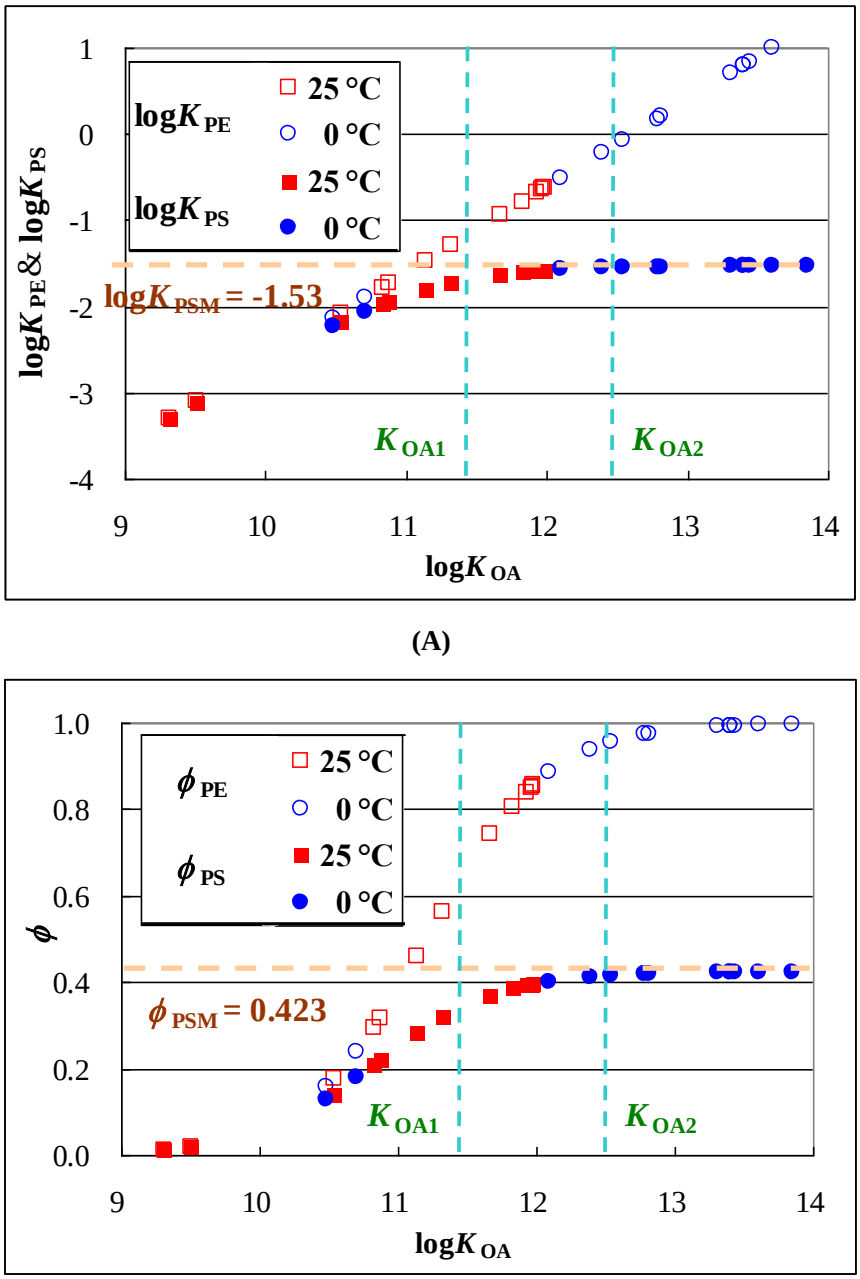

(A)

(B)

Figure S17: **(A)** Partition coefficients of 11 PBDE congeners (BDE-17, -28, -66, -77, -99, -100, -126, -153, -154, -156, and -183) at 25 ℃ and 0 ℃ calculated using Eq. (3) for equilibrium and Eq. (31) for steady state (Assuming f_{OM} = 0.2). **(B)** Particle fraction of the 11 PBDE congeners at 25 ℃ and 0 ℃ calculated using Eq. (41) from the data shown in (A) (Assuming *TSP* = 25 μg/m^3). The source for the results under equilibrium: Harner and Shoeib (2002). The values of logK_{OA} for the 11 PBDE congeners were calculated by using Eq. (**7**).

Figure S18: Sampling site Waliguan. Our air sampler was installed on the top of the building (Photo was taken by Yi-Fan Li).

Supplementary Tables

Table S1: Parameters *A* and *B* for PBDEs, used to calculate logK_{OA} (logK_{OA} = $A+B/(t+273.15)$) (Harner and Shoeib, 2002).

PBDE Congener	*A*	*B*
BDE-17	-3.45	3803
BDE-28	-3.54	3889
BDE-47	-6.47	5068
BDE-66	-7.88	5576
BDE-77	-5.69	4936
BDE-85	-6.22	5331
BDE-99	-4.64	4757
BDE-100	-7.18	5459
BDE-126	-8.41	6077
BDE-153	-5.39	5131
BDE-154	-4.62	4931
BDE-156	-5.8	5298
BDE-183	-3.71	4672

References

Cetin, B. and Odabasi, M.: Atmospheric concentrations and phase partitioning of polybrominated diphenyl ethers (PBDEs) in Izmir, Turkey. Chemosphere 71, 1067-1078, 2007.

Harner, T. and Bidleman, T. F.: Octanol - air partition coefficient for describing particle/gas partitioning of aromatic compounds in urban air. Environ. Sci. Technol., 32, 1494-1502, 1998.

Harner, T. and Shoeib, M.: Measurements of octanol - air partition coefficients (K_{OA}) for polybrominated diphenyl ethers (PBDEs): Predicting partitioning in the environment. J. Chem. Eng. Data 47, 228-232, 2002.

Hayakawa K, Takatsuki H, Watanabe I, Sakai S.: Polybrominated diphenyl ethers (PBDEs), polybrominated dibenzo-p-dioxins/dibenzofurans (PBDD/Fs) and monobromo-polychlorinated dibenzo-p-dioxins/dibenzofurans (MoBPXDD/Fs) in the atmosphere and bulk deposition in Kyoto, Japan. Chemosphere, 57, 343-356, 2004.

Li Y. F. and Jia, H. L.: Prediction of gas/particle partition quotients of polybrominated diphenyl ethers (PBDEs) in north temperate zone air: An empirical approach. Ecotoxic. Environ. Safety, 108, 65-71, 2014.

Mackay, D. 2001. Multimedia Environmental Models: The Fugacity Approach, 2nd Edition, Taylor & Francis, New York. p:261

Möller, A, Xie, Z, Sturm R, and Ebinghaus, R.: Polybrominated diphenyl ethers (PBDEs) and alternative brominated flame retardants in air and seawater of the European Arctic. Environ. Pollut. 159, 1577-1583, 2011.

NCP 2013: Canadian Arctic Contaminants Assessment Report On Persistent Organic Pollutants – 2013 (eds Muir D, Kurt-Karakus P, Stow J.). (Northern Contaminants Program, Aboriginal Affairs and Northern Development Canada, Ottawa ON. xxiii + 487 pp + Annex 2013.

Strandberg, B., Dodder, N. G., Basu, I., and Hites, R. A.: Concentrations and Spatial Variations of Polybromin ated Diphenyl Ethers and Other Organohalogen Compounds in Great Lakes Air. Environ. Sci. Technol., 35, 1078-1083, 2001.

Tian, M., Chen, S., Wang, J., Zheng, X., Luo, X., and Mai, B.: Brominated Flame Retardants in the Atmosphere of E-Waste and Rural Sites in Southern China: Seasonal Variation, Temperature Dependence, and Gas-Particle Partitioning

Environ. Sci. Technol., 45, 8819-8825, 2011.

Yang, M., Qi, H., Jia, H., Ren, N., Ding, Y., Ma, W., Liu, L., Hung, H., Sverko, E., and Li, Y. F.: Polybrominated Diphenyl Ethers (PBDEs) in Air across China: Levels, Compositions, and Gas-Particle Partitioning. Environ Sci Technol, 47, 8978-8984, 2013.